THE JOURNAL OF PHYSICAL CHEMISTRY B
A JOURNAL OF THE AMERICAN CHEMICAL SOCIETY

pubs.acs.org/JPCB

Article

Lack of Correlation between Landscape Geometry and Transition Rates

Published as part of The Journal of Physical Chemistry virtual special issue "Jose Onuchic Festschrift".

Wen Jia, Atchuta Srinivas Duddu, Mohit Kumar Jolly, and Herbert Levine*

Cite This: *J. Phys. Chem. B* 2022, 126, 5613–5618

Read Online

ACCESS | Metrics & More | Article Recommendations

ABSTRACT: Biological cells can exist in a variety of distinct phenotypes, determined by the steady-state solutions of genetic networks governing their cell fate. A popular way of representing these states relies on the creation of landscape related to the relative occupation of these states. It is often assumed that this landscape offers direct information regarding the state-to-state transition rates, suggesting that these are related to barrier heights separating landscape minima. Here, we study a toggle triad network exhibiting multistability and directly demonstrate the lack of any direct correlation between properties of the landscape and corresponding transition rates.

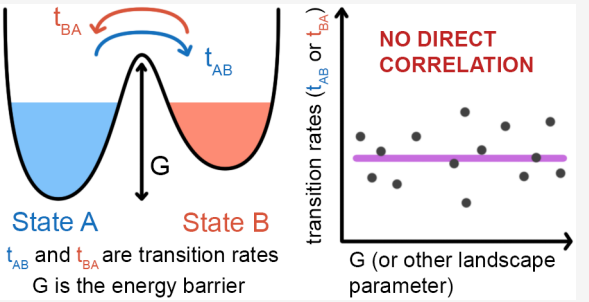

INTRODUCTION

Cell fate transitions form an essential part of developmental processes and also have been shown to play a critical role in cancer metastasis. These transitions occur between cells of differing phenotype, commonly thought of as arising due to multistability in the genetic networks governing gene expression. The simplest such decisions take place between binary choices, such as hematopoietic stem cells differentiating into either myeloid or lymphatic progenitors.[1] Increasingly, however, it has been recognized that cells can exhibit higher-order multistability, leading for example to hybrid E/M states during the epithelial-mesenchymal transition (EMT)[2−5] or the formation of mixed Th1/Th2 T-cells from T-helper cell precursors.[6] We note that the dynamics of such systems are nonequilibrium, which means that the deterministic terms are not derivable from a free energy and the dynamics does not obey detailed balance.

One of the methods that has been widely used to represent stochastic dynamical processes with multiple steady-state solutions in their deterministic limit relies on the determination of an effective "energy" landscape.[7−9] This landscape is defined by the probability distribution P of being at a particular point in the space spanned by the dynamical variables via $U = -\ln P$. This definition is designed such that in a system in thermodynamic equilibrium, U is just the free energy of a given configuration. In the landscape, steady-states appear as local minima, i.e. as locations with high probability; various realizations of the process get stuck for long periods of time in the regions around these states, thereby giving rise to large P and small U. Again, this is supposed to be analogous to what happens in equilibrium systems, where macroscopic systems with small fluctuations flock to configurations of minimal free energy.

In a bistable system, there is of necessity a simple connection between the effective landscape and the notion of transition probability. Imagine decomposing the configuration space into two regions, defined by the basins of attraction of the two fixed points, e.g., A_b and B_b of A and B respectively, of the deterministic limit dynamics. If we define r_{AB} as the rate to go from region A_b to region B_b and r_{BA} as the reverse, it is clear that the once the stochastic process reaches a steady-state, we will approximately have the balance $r_{AB}P(A) = r_{BA}P(B)$. The approximation will become increasingly accurate as the noise becomes smaller and the deterministic rates of attraction to the fixed points becomes much larger than the transition rates and hence the minima become increasingly sharp and the difference between the probabilities is dominated by the peak height difference. This is again familiar from the equilibrium context, where simple arguments predict $r_{AB} \sim \exp(U(A) - U_t)$, $r_{BA} \sim \exp(U(B) - U_t)$, where U_t is the free energy of the transition state, i.e. the minimum value of maximal free energy along the path from A to B as we vary among paths. This leads immediately to the aforementioned balance result.

Received: April 24, 2022
Revised: July 8, 2022
Published: July 25, 2022

https://doi.org/10.1021/acs.jpcb.2c02837
J. Phys. Chem. B 2022, 126, 5613−5618

It is quite natural to hope that this strong connection between the effective landscape and the transitions among phenotypes would be true in general, i.e., for multistable systems. In fact, this assumption seems to be implicit in many discussions of phenotypic landscapes in the biological literature.[10−12] For example, a recent review argues that the landscape is "canalized" into specific basins of attraction, defining low-energy paths that connect attractor states to each other.[13] This is certainly the picture that emerges from a cursory glance at the famous Waddington drawing of the developmental process. However, this is not correct in general, as (using an old aphorism) is well-known to those who know it well.[14−16] This is because, as is pointed out in several papers, landscapes do not in general uniquely determine dynamics of nonequilibrium systems and must be augmented by the knowledge of various fluxes, corresponding to nongradient flows. Specifically, there is still a unique transition path which determines the rate at low noise, but it is not the one given by relaxation on the aforementioned effective potential U; instead, it can be determined by minimizing the action defined by Wentzell and Friedlin.[17] In particular, the path that dominates does not go through the saddle points of the landscape-based potential,[18] and hence there is no reason any feature of this point should automatically control the transition rate. Various papers,[19] including one by Onuchic and co-workers,[20] derive the correct approaches to solving this problem. However, the messages from these works are somewhat complicated and hence not fully appreciated and hence this paper.

Here, we use a simple network exhibiting tristability to investigate the landscape−transition rate connection. Our model is a stochastic version of toggle-switch triad as has been studied,[21] and we computationally determine both the probability distribution and the transition rates and show that the former does not directly determine the latter. We then discuss the implications of our findings for the proper use versus misuse of the landscape concept in the cell biology context.

RESULTS

Toggle Triad Network Can Give Rise to a Balanced Tristable System. The toggle switch model is widely used as a simple example of a network with mutually inhibiting proteins whose interaction create multistability.[6] Here, we study a toggle triad network where all three proteins inhibit each other (Figure 1) and determine parameters (through the use of RACIPE[22]) such that the ODE reaction system exhibits three stable states: state A (high A, low B, low C), state B (low A, high B, low C), and state C (low A, low B, high C) with relatively equal basins of attraction; for simplicity we have referred to these states by the protein with highest concentration, namely A, B, or C. We generated 100 randomly chosen initial conditions for a variety of parameter sets and tracked which final state would be converged to. For our chosen parameter set, this calculation found gives 42 cases of convergence to state A, 33 cases to state B, and 25 cases to state C, which indicates the three states can be considered balanced.

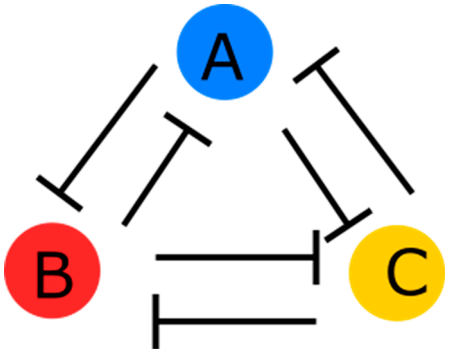

Figure 1. Toggle triad network. The network consists of three proteins (A, B and C); each protein mutually inhibits each of the other two.

Next, we added noise to the ODE dynamics simulation for the same parameter set, in order to trigger transitions between different states; typical results are shown in (Figure 2). A high level of the blue line indicates that the system in state A, a high level of the red line implies state B and high level of yellow line implies state C. Thus, our stochastic toggle triad network successfully generates a tristable system, and serves as a simple testbed for concepts to be applied to more complex genetic networks that have been shown to generate three stable phenotypes.[3,23−30]

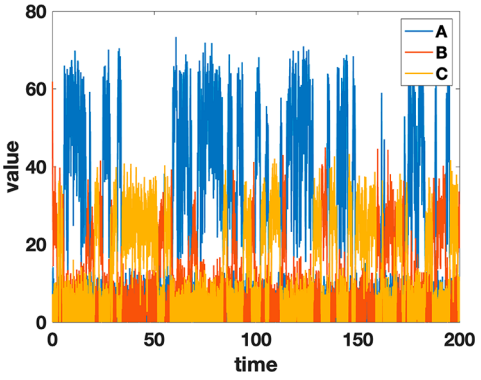

Figure 2. Dynamic simulation of the toggle triad network. Independent white noise was added to the three governing ODEs in order to trigger transitions between states. The noise is Gaussian distributed with mean zero and standard deviation 40 and is added every time step of duration 0.01. The times at which the highest curve is blue indicates that the system is in state A, red high represents state B, and yellow high represents state C.

Energy Landscape and Flux. We can plot the effective landscape, based on our dynamic simulations. A PCA heatmap clearly shows the expected three stable states (Figure 3a). We also carried out probability flux analysis (PFA)[31] to track the dynamical flow of flux in our network (Figure 3b). One can clearly see the presence of rotational components of the flow, for example in the region around fixed-point C. This is a general consequence of the fact that the ODE model cannot be written as a gradient flow.

We wish to connect this structure to a reduced Markov transition description that focuses on the probability of being in a particular state and the transition rates between them. In order to determine the state of a specific point (A, B, C) in concentration space, we carry out a deterministic ODE integration simulation starting at this point (A, B, or C) and determine its final stable state. Via this procedure, the basins of attraction can be mapped out and all the combinations of the (A, B, C) concentrations can be classified into one of the three states, A, B, or C. Then, by integrating the probability P over each of these regions, we obtain the effective potential of a

https://doi.org/10.1021/acs.jpcb.2c02837
J. Phys. Chem. B 2022, 126, 5613−5618

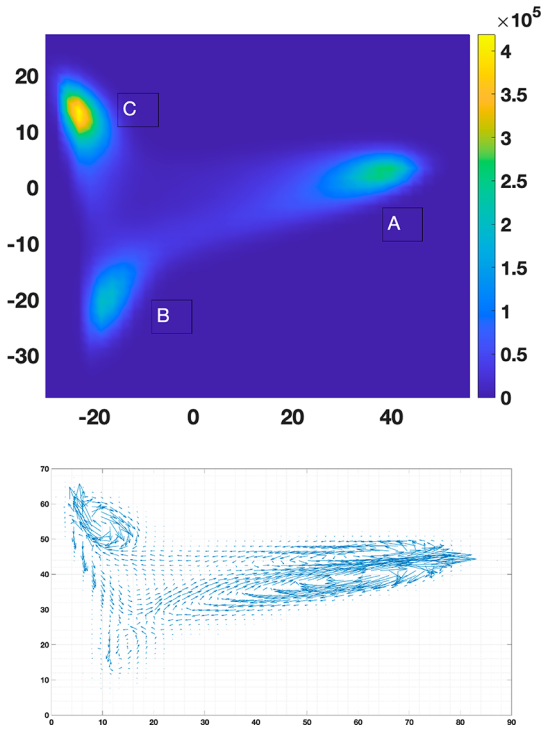

Figure 3. (A) PCA (principal component analysis) for toggle triad network, by reducing the dimensionality of 3D (A, B, C) data sets to 2D. The three stable states are labeled. (B) PFA (probability flux analysis) for toggle triad network. This is done based on PCA results, and blue arrows indicate the direction of flux between three states.

specific state i can be defined as $U_i = -\ln P_i$ where P is the probability of being in state i. The results are given in Table 1.

Table 1. Probability and Corresponding Effective Potential of Three States

P_A	P_B	P_C
0.44	0.20	0.36
U_A	U_B	U_C
0.82	1.61	1.02

From the effective potential we calculated (Table 1), we might roughly expect that since P_A has the largest value, transiting out of state A is harder than out of state B or state C. We will see below that this intuition can be confirmed. On the other hand, one might also have the intuition that the rate of transitioning from, for example, state A to state B would be directly governed by the barrier between them as determined by the effective potential; high walls would automatically mean low transition rates. As already mentioned, this is the impression left by the famous Waddington landscape picture,[32,33] where the walls between phenotypes get progressively higher during development, supposedly representing the stabilization of increasing differentiated cell types. Is this intuition in fact accurate?

Transition Rates Calculation. To test the connection between rates and the effective landscape, we turn to a coarse-grained Markov model description of the phenotypic dynamics in our system. Focusing on the temporal evolution of the state of the system, the master equations of a reduced model can be written as

$$\dot{P}_A = -(r_{AB} + r_{AC})P_a + r_{BA}P_B + r_{CA}P_C$$

$$\dot{P}_B = r_{AB}P_A - (r_{BA} + r_{BC})P_B + r_{CB}P_C$$

$$\dot{P}_C = r_{AC}P_A + r_{BC}P_B - (r_{CA} + r_{CB})P_C$$

Considering a start from A, we can track the time it takes to reach state B or C and calculate the transition rates based on the probability distribution:

$$p_{AB}(t) = r_{AB}e^{-(r_{AB}+r_{AC})t}$$

$$p_{AC}(t) = r_{AC}e^{-(r_{AB}+r_{AC})t}$$

We performed the stochastic dynamic simulation as we discussed above, and obtained the probability distribution by fitting the histogram (i.e., the time it took to go from A to B or C). Here, we only fit the decay part of the curve (Figure 4); the Markov model predicts a single exponential decay, which cannot be precisely correct for our stochastic ODE simulations, as it always takes some finite time to go from the initial starting point at the peak to a different state. From the figure, we see that this issue only affects the smallest time bin. Once the rate

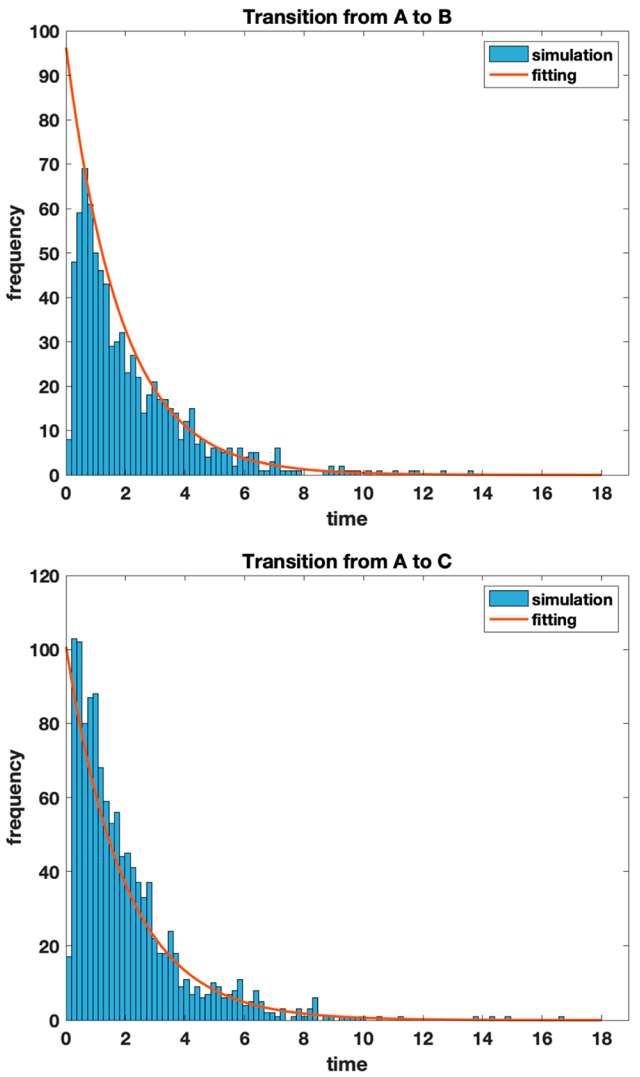

Figure 4. Probability distribution of transition times going from A to B and from A to C.

https://doi.org/10.1021/acs.jpcb.2c02837
J. Phys. Chem. B 2022, 126, 5613−5618

Table 2. All the Calculations for the Baseline Parameter Set 1

state	state probability	potential	transition rate	potential difference	log of rate
A	0.44	0.82	r_{AB}: 0.27 r_{AC}: 0.26	$U_A - U_B$: 0.79	$\ln r_{AB}/r_{BA}$: 1.36
B	0.20	1.61	r_{BA}: 1.05 r_{BC}: 0.002	$U_B - U_c$: −0.59	$\ln r_{BC}/r_{CB}$: 4.65
C	0.36	1.02	r_{CA}: 0.31 r_{CB}: 0.21	$U_C - U_A$: −0.20	$\ln r_{CA}/r_{AC}$: −0.18

sum is determined from the overall exponential decay, the ratio of the rates is just the ratio of the two coefficients of the exponential fit.

Similarly, we also fitted the probability distribution curve for the rates leaving states B and C. All of the corresponding calculated transition rates are shown in Table 2. Our results do satisfy the intuitive relationship mentioned above that

$$r_{AB} + r_{AC} < r_{BC} + r_{BA}$$
$$r_{AB} + r_{AC} < r_{CA} + r_{CB}$$

Table 3. Probability Comparisons for Two Parameter Set

	set no. 1			set no. 2	
	P_{sol}	P_{ODE}		P_{sol}	P_{ODE}
A	0.54	0.44	A	0.56	0.53
B	0.19	0.20	B	0.30	0.40
C	0.28	0.36	C	0.15	0.07

However, the barrier height idea is demonstrably incorrect. From the argument presented in introduction, if the correlation

$$r_{AB} \sim \exp(U(\mathrm{A}) - U_t)$$
$$r_{BA} \sim \exp(U(\mathrm{B}) - U_t)$$

is correct, it can be easily derived that

$$\ln\frac{r_{AB}}{r_{BA}} \cong U(\mathrm{A}) - U(\mathrm{B})$$
$$\ln\frac{r_{CA}}{r_{AC}} \cong U(\mathrm{C}) - U(\mathrm{A})$$
$$\ln\frac{r_{BC}}{r_{CB}} \cong U(\mathrm{B}) - U(\mathrm{C})$$

We calculated these values, and they are listed in Table 2. As the results show here, the logarithm of transition rate ratio is not correctly given by the potential energy difference. In general, our calculation directly reveals the lack of correlation between the landscape picture and the transition rates.

More quantitatively, we need to determine how accurate is our three-state reduction approach as compared to the ODE model. We can solve the three-state model exactly and determine that

$$P_{A\_sol} = \frac{r_{BA}r_{CB} + r_{CA}r_{BA} + r_{CA}r_{BC}}{r_{BA}r_{CB} + r_{CA}r_{BA} + r_{CA}r_{BC}r_{AB}r_{CA} + r_{CB}r_{AB} + r_{CB}r_{AC}r_{BC}r_{AB} + r_{AC}r_{BC} + r_{AC}r_{BA}}$$
$$P_{B\_sol} = \frac{r_{AB}r_{CA} + r_{CB}r_{AB} + r_{CB}r_{AC}}{r_{BA}r_{CB} + r_{CA}r_{BA} + r_{CA}r_{BC}r_{AB}r_{CA} + r_{CB}r_{AB} + r_{CB}r_{AC}r_{BC}r_{AB} + r_{AC}r_{BC} + r_{AC}r_{BA}}$$
$$P_{C\_sol} = \frac{r_{BC}r_{AB} + r_{AC}r_{BC} + r_{AC}r_{BA}}{r_{BA}r_{CB} + r_{CA}r_{BA} + r_{CA}r_{BC}r_{AB}r_{CA} + r_{CB}r_{AB} + r_{CB}r_{AC}r_{BC}r_{AB} + r_{AC}r_{BC} + r_{AC}r_{BA}}$$

We compared these probabilities (P_{sol}) with the probability obtained from the ODE simulations (P_{ODE}) for our basic parameter set (Table 3) as well as one additional set (see Appendix). The probability values are reasonably close to each other, which shows that our model reduction is accurate with the error averaging about 20%.

This then allows to compute the ratio of the rate products going the two ways around the ABC loop. The landscape approach as indicated by the above relationships automatically gives unity for this ratio. From the transition rates in Table 2, we have

$$r_{AC} \times r_{CB} \times r_{BA} = 0.26 \times 0.21 \times 1.05 = 0.05733$$
$$r_{CA} \times r_{BC} \times r_{AB} = 0.31 \times 0.002 \times 0.27 = 0.00017$$

This is obviously very far outside the range that would be expected given the 20% average error. In other words, the balanced triad model has nonzero flux, a clear indicator that the landscape picture is not capable of describing the model dynamics.

Parenthetically, we note that for the second parameter set, the ODE simulations show that there are no transitions from B to C or C to B that do not go through A as an obligate intermediate. This structure explicitly prevents nonzero flux, and for this special condition, the landscape picture is sufficient.

DISCUSSION

In many research papers (see ref 13 and references therein), it is implicitly assumed that the height of the barrier between states as computed from the effective energy $U = -\ln P$ is proportional to the negative logarithm of the transition rate between two states. This is indicated directly in the often-reproduced Waddington picture, where the heights of the walls are supposed to represent the increasing lack of plasticity of cell phenotypes as development progresses. In order to show that this concept is in general untrue, we adopted a simple but powerful model, the toggle triad network, which has three distinct stable states and which can be easily simulated as well as analyzed.[21] We note that there may be some real biological

https://doi.org/10.1021/acs.jpcb.2c02837
J. Phys. Chem. B 2022, 126, 5613−5618

systems that are accurately modeled by the toggle triad system,[34] but this is not directly relevant in terms of our general conclusion.

Of course, what is true generically for dynamical systems may not be the case for a specific biological system, as shaped by evolution. Thus, some authors have constructed models of gene networks that do have dynamics that arise from a "energy" minimization, i.e., behave like equilibrium systems.[35,36] When this very strong assumption will prove to be actually correct is an interesting question for future research.

APPENDIX

In the Results, we calculated the transition rates between states by fitting the probability distribution curve. In order to show that this method works, we used the Gillespie algorithm to perform a biochemical reaction simulation, which was given the specific reaction rates. Then, we calculated its reaction rates by fitting the simulated probability distribution. The calculated reaction rates are very close to the given rates (Table 4).

Table 4. Reaction Rates Comparison

	r_{AB}	r_{BC}	r_{CA}	r_{BA}	r_{CB}	r_{AC}
input	0.0116	0.1101	0.0088	0.0125	0.0225	0.1773
output	0.0135	0.1121	0.0107	0.0120	0.0241	0.1995

Table 5. All of the Parameters for Set No. 1 (Baseline Set)

	production rate		degradation rate
A	42.68		0.67
B	7.39		0.25
C	16.68		0.62
effect from X to Y	threshold X_Y^0	binding no. n_{XY}	fold change λ_{XY}
inhibition from A to B	9.79	2	0.01
inhibition from A to C	11.07	2	0.01
inhibition from B to A	9.23	4	0.03
inhibition from B to C	10.20	6	0.01
inhibition from C to A	7.93	6	0.03
inhibition from C to B	9.09	4	0.01

Table 6. All of the Parameters for Set No. 2

	production rate		degradation rate
A	56.76		0.61
B	30.27		0.43
C	54.85		0.47
effect from X to Y	threshold X_Y^0	binding no. n_{XY}	fold change λ_{XY}
inhibition from A to B	5.58	3	0.02
inhibition from A to C	11.24	2	0.01
inhibition from B to A	6.19	3	0.01
inhibition from B to C	2.30	4	0.02
inhibition from C to A	8.79	4	0.09
inhibition from C to B	9.75	5	0.04

Next, we present the details of our ODE model. The ODEs for our triad toggle switch are

$$\dot{A} = g_A \times H_B^S \times H_C^S - k_A \times A$$

$$\dot{B} = g_B \times H_A^S \times H_C^S - k_B \times B$$

$$\dot{C} = g_C \times H_A^S \times H_B^S - k_C \times C$$

Here, H^S is the shifted Hill function defined as

$$H_X^S = H_X^- + \lambda H_X^+$$

$$H_X^- = \frac{1}{1 + \left(\frac{X}{X_0}\right)^{n_X}}$$

$$H_X^+ = 1 - H_X^-$$

where λ is the fold change from the basal synthesis rate due to protein X. For activators, $\lambda > 1$, and for inhibitors, $\lambda < 1$.

The specific parameters we used for set no. 1 and set no. 2 are given in Tables 5 and 6.

AUTHOR INFORMATION

Corresponding Author

Herbert Levine − *Center for Theoretical Biological Physics, Northeastern University, Boston, Massachusetts 02115, United States; Department of Bioengineering and Department of Physics, Northeastern University, Boston, Massachusetts 02115, United States;* orcid.org/0000-0002-8819-9055; Email: h.levine@northeastern.edu

Authors

Wen Jia − *Center for Theoretical Biological Physics, Northeastern University, Boston, Massachusetts 02115, United States; Department of Physics and Astronomy, Rice University, Houston, Texas 77005, United States*

Atchuta Srinivas Duddu − *Centre for BioSystems Science and Engineering, Indian Institute of Science, Bangalore 560012, India*

Mohit Kumar Jolly − *Centre for BioSystems Science and Engineering, Indian Institute of Science, Bangalore 560012, India*

Complete contact information is available at: https://pubs.acs.org/10.1021/acs.jpcb.2c02837

Notes

The authors declare no competing financial interest.

ACKNOWLEDGMENTS

The work of W.J. and H.L. was supported by the National Science Foundation sponsored Center for Theoretical Biological Physics, Award PHY-2019745, and by PHY-1605817. M.K.J. was supported by the Ramanujan Fellowship awarded by SERB, DST, Government of India (SB/S2/RJN-049/2018). A.S.D. was supported by the Prime Ministers' Research Fellowship (PMRF), Government of India.

REFERENCES

(1) Mojtahedi, M.; Skupin, A.; Zhou, J.; Castaño, I. G.; Leong-Quong, R. Y. Y.; Chang, H.; Trachana, K.; Giuliani, A.; Huang, S. Cell Fate Decision as High-Dimensional Critical State Transition. *PLOS Biology* **2016**, *14* (12), No. e2000640.

(2) Nieto, M. A.; Huang, R. Y.-J.; Jackson, R. A.; Thiery, J. P. EMT: 2016. *Cell* **2016**, *166* (1), 21−45.

(3) Jolly, M. K.; Boareto, M.; Huang, B.; Jia, D.; Lu, M.; Ben-Jacob, E.; Onuchic, J. N.; Levine, H. Implications of the Hybrid Epithelial/Mesenchymal Phenotype in Metastasis. *Frontiers in Oncology* **2015**, *5*, 0155.

(4) Yu, M.; Bardia, A.; Wittner, B. S.; Stott, S. L.; Smas, M. E.; Ting, D. T.; Isakoff, S. J.; Ciciliano, J. C.; Wells, M. N.; Shah, A. M.; Concannon, K. F.; Donaldson, M. C.; Sequist, L. V.; Brachtel, E.; Sgroi, D.; Baselga, J.; Ramaswamy, S.; Toner, M.; Haber, D. A.;

Maheswaran, S. Circulating Breast Tumor Cells Exhibit Dynamic Changes in Epithelial and Mesenchymal Composition. *Science* **2013**, *339* (6119), 580−584.
(5) Armstrong, A. J.; Marengo, M. S.; Oltean, S.; Kemeny, G.; Bitting, R. L.; Turnbull, J. D.; Herold, C. I.; Marcom, P. K.; George, D. J.; Garcia-Blanco, M. A. Circulating Tumor Cells from Patients with Advanced Prostate and Breast Cancer Display Both Epithelial and Mesenchymal Markers. *Molecular Cancer Research* **2011**, *9* (8), 997−1007.
(6) Huang, S. Hybrid T-Helper Cells: Stabilizing the Moderate Center in a Polarized System. *PLOS Biology* **2013**, *11* (8), No. e1001632.
(7) Wang, J.; Verkhivker, G. M. Energy Landscape Theory, Funnels, Specificity, and Optimal Criterion of Biomolecular Binding. *Phys. Rev. Lett.* **2003**, *90* (18), 188101.
(8) Kim, K.-Y.; Wang, J. Potential Energy Landscape and Robustness of a Gene Regulatory Network: Toggle Switch. *PLOS Computational Biology* **2007**, *3* (3), No. e60.
(9) Yang, S.; Onuchic, J. N.; Levine, H. Effective stochastic dynamics on a protein folding energy landscape. *J. Chem. Phys.* **2006**, *125* (5), 054910.
(10) Sáez, M.; Blassberg, R.; Camacho-Aguilar, E.; Siggia, E. D.; Rand, D. A.; Briscoe, J. Statistically derived geometrical landscapes capture principles of decision-making dynamics during cell fate transitions. *Cell Systems* **2022**, *13* (1), 12−28.
(11) Jin, S.; MacLean, A. L.; Peng, T.; Nie, Q. scEpath: Energy landscape-based inference of transition probabilities and cellular trajectories from single-cell transcriptomic data. *Bioinformatics* **2018**, *34* (12), 2077−2086.
(12) Paudel, B. B.; Harris, L. A.; Hardeman, K. N.; Abugable, A. A.; Hayford, C. E.; Tyson, D. R.; Quaranta, V. A Nonquiescent "Idling" Population State in Drug-Treated, BRAF-Mutated Melanoma. *Biophys. J.* **2018**, *114* (6), 1499−1511.
(13) Teschendorff, A. E.; Feinberg, A. P. Statistical mechanics meets single-cell biology. *Nat. Rev. Genet.* **2021**, *22* (7), 459−476.
(14) Wang, J.; Xu, L.; Wang, E. Potential landscape and flux framework of nonequilibrium networks: Robustness, dissipation, and coherence of biochemical oscillations. *Proc. Natl. Acad. Sci. U. S. A.* **2008**, *105* (34), 12271−12276.
(15) Wang, J. Landscape and flux theory of non-equilibrium dynamical systems with application to biology. *Adv. Phys.* **2015**, *64* (1), 1−137.
(16) Zhou, J. X.; Aliyu, M. D. S.; Aurell, E.; Huang, S. Quasi-potential landscape in complex multi-stable systems. *Journal of The Royal Society Interface* **2012**, *9* (77), 3539−3553.
(17) Freidlin, M. I.; Wentzell, A. D. Random Perturbations of Dynamical Systems. *Studies in Math*; 1984; Vol. *260*.
(18) Feng, H.; Zhang, K.; Wang, J. Non-equilibrium transition state rate theory. *Chemical Science* **2014**, *5* (10), 3761−3769.
(19) Maier, R. S.; Stein, D. L. Transition-rate theory for nongradient drift fields. *Physical review letters* **1992**, *69* (26), 3691.
(20) Lu, M.; Onuchic, J.; Ben-Jacob, E. Construction of an Effective Landscape for Multistate Genetic Switches. *Phys. Rev. Lett.* **2014**, *113* (7), 078102.
(21) Duddu, A. S.; Sahoo, S.; Hati, S.; Jhunjhunwala, S.; Jolly, M. K. Multi-stability in cellular differentiation enabled by a network of three mutually repressing master regulators. *Journal of The Royal Society Interface* **2020**, *17* (170), 20200631.
(22) Huang, B.; Jia, D.; Feng, J.; Levine, H.; Onuchic, J. N.; Lu, M. RACIPE: A computational tool for modeling gene regulatory circuits using randomization. *BMC Systems Biology* **2018**, *12* (1), 74.
(23) Duddu, A. S.; Majumdar, S. S.; Sahoo, S.; Jhunjhunwala, S.; Jolly, M. K. Emergent dynamics of a three-node regulatory network explain phenotypic switching and heterogeneity: A case study of Th1/Th2/Th17 cell differentiation. *Mol. Biol. Cell* **2022**, *33*, E21-10-0521.
(24) Jia, D.; Jolly, M. K.; Harrison, W.; Boareto, M.; Ben-Jacob, E.; Levine, H. Operating principles of tristable circuits regulating cellular differentiation. *Physical Biology* **2017**, *14* (3), 035007.
(25) Jia, D.; Jolly, M. K.; Tripathi, S. C.; Den Hollander, P.; Huang, B.; Lu, M.; Celiktas, M.; Ramirez-Peña, E.; Ben-Jacob, E.; Onuchic, J. N.; Hanash, S. M.; Mani, S. A.; Levine, H. Distinguishing mechanisms underlying EMT tristability. *Cancer Convergence* **2017**, *1* (1), 2.
(26) Lu, M.; Jolly, M. K.; Levine, H.; Onuchic, J. N.; Ben-Jacob, E. MicroRNA-based regulation of epithelial-hybrid-mesenchymal fate determination. *Proc. Natl. Acad. Sci. U. S. A.* **2013**, *110* (45), 18144−18149.
(27) Tripathi, S.; Chakraborty, P.; Levine, H.; Jolly, M. K. A mechanism for epithelial-mesenchymal heterogeneity in a population of cancer cells. *PLOS Computational Biology* **2020**, *16* (2), No. e1007619.
(28) Jia, W.; Deshmukh, A.; Mani, S. A.; Jolly, M. K.; Levine, H. A possible role for epigenetic feedback regulation in the dynamics of the Epithelial-Mesenchymal Transition (EMT). *Physical Biology* **2019**, *16* (6), 066004.
(29) Lu, M.; Jolly, M. K.; Gomoto, R.; Huang, B.; Onuchic, J.; Ben-Jacob, E. Tristability in Cancer-Associated MicroRNA-TF Chimera Toggle Switch. *J. Phys. Chem. B* **2013**, *117* (42), 13164−13174.
(30) Tian, X.-J.; Zhang, H.; Xing, J. Coupled Reversible and Irreversible Bistable Switches Underlying TGFβ-induced Epithelial to Mesenchymal Transition. *Biophys. J.* **2013**, *105* (4), 1079−1089.
(31) Battle, C.; Broedersz, C. P.; Fakhri, N.; Geyer, V. F.; Howard, J.; Schmidt, C. F.; MacKintosh, F. C. Broken detailed balance at mesoscopic scales in active biological systems. *Science* **2016**, *352* (6285), 604−607.
(32) Wang, J.; Zhang, K.; Xu, L.; Wang, E. Quantifying the Waddington landscape and biological paths for development and differentiation. *Proc. Natl. Acad. Sci. U. S. A.* **2011**, *108* (20), 8257−8262.
(33) Van Speybroeck, L. From Epigenesis to Epigenetics. *Ann. N.Y. Acad. Sci.* **2002**, *981* (1), 61−81.
(34) Fang, D.; Zhu, J. Dynamic balance between master transcription factors determines the fates and functions of CD4 T cell and innate lymphoid cell subsets. *Journal of Experimental Medicine* **2017**, *214* (7), 1861−1876.
(35) Rand, D. A.; Raju, A.; Sáez, M.; Corson, F.; Siggia, E. D. Geometry of gene regulatory dynamics. *Proc. Natl. Acad. Sci. U. S. A.* **2021**, *118* (38), No. e2109729118.
(36) Lang, A. H.; Li, H.; Collins, J. J.; Mehta, P. Epigenetic Landscapes Explain Partially Reprogrammed Cells and Identify Key Reprogramming Genes. *PLOS Computational Biology* **2014**, *10* (8), No. e1003734.

https://doi.org/10.1021/acs.jpcb.2c02837
J. Phys. Chem. B 2022, 126, 5613−5618